

Development of Medium-Frequency Molded Transformer for SST with Simultaneous Insulation and Forced Air-Cooling capabilities

Ritsuki Yonetomi, Keisuke Kusaka
Nagaoka University of Technology
1603-1, Kamitomioka-machi, Nagaoka
Niigata, Japan

Tel.: +81 / (258) – 47 – 9622

E-Mail: s213194@stn.nagaokaut.ac.jp, kusaka@vos.nagaokaut.ac.jp

URL: <https://eclab01.nagaokaut.ac.jp/>

Acknowledgements

This paper is based on results obtained from a project commissioned by the New Energy and Industrial Technology Development Organization (NEDO) (JPNP14004).

Keywords

«Solid-state transformer», «Transformer», «DC/DC converter», «Partial discharge», «Insulation».

Abstract

This paper proposes a new plastic mold structure for medium-frequency molded transformers used in solid-state transformers (SSTs), aiming to enhance both the cooling performance of windings and insulation capabilities. In medium-frequency transformers for 6.6-kV SST, high-voltage insulation performance is required between the primary and secondary windings. Therefore, insulation should be provided by molding around the windings. In contrast, an effective cooling method for windings is necessary because copper losses in the windings also increase as the operating frequency rises.

In this paper, temperature rise in the windings, which is a problem in medium-frequency molded transformers, is addressed by applying plastic molding only to the high electric field generating part in a structure that allows efficient cooling. Experimental results show that the developed transformer, which has a power density of 12.6 kW/L, continuously transmit 37.5 kW with a maximum transmission efficiency of 99.2%. In addition, partial discharge tests of the developed transformer show that it has sufficient insulation performance for SST with a 6.6-kV input.

Introduction

In recent years, solid-state transformers (SSTs) with the ability to reduce transformer volume by operating at medium or high frequency, have gained attention as a replacement for transformers in DC smart grids or commercial-frequency transformers in ultra-rapid electric vehicle chargers. SSTs decrease transformer size by operating at medium or high frequencies. In addition, features such voltage regulation, reactive power compensation, and the integration of energy storage systems in multi-cell configurations—capabilities that conventional commercial-frequency transformers cannot provide—will also be implemented [1–2].

Regarding SST topology, a multi-cell system with multiple cells connected in series on the input side and in parallel on the output side — known as input-series, output parallel connection (ISOP) — has been proposed. Each cell contains a DC/DC converter with a transformer that operates at medium or high frequency. Consequently, this configuration plays a crucial role in delivering the required voltage to the load through isolation and voltage conversion [3]. The ISOP connection reduces the voltage applied to the primary and secondary sides of a high-frequency transformer, making it possible to reduce transformer volume significantly. However, a maximum voltage of 6.6 kV is applied between the transformer's primary and secondary windings for a 6.6-kV AC grid. This means high insulation performance between the windings and demands must be ensured [4].

As an insulation degradation phenomenon in equipment subjected to high voltage, partial discharge (PD) is known. PD is one of the causes of long-term degradation of the insulation performance of transformers. When there are minute defects called voids in the insulation material installed between the windings to which

high voltage is applied, PD occurs due to the transfer of minute electrical charges through these voids [5]. PD causes deterioration of the transformer's insulation material, shortening the life of the insulation and leading to premature failure [6–8]. PD testing is used to improve the insulation reliability of high-voltage equipment [9]. PD testing detects minute electrical charges when high voltages are applied to insulators and can estimate the risk of deterioration of insulating materials [10–11].

Therefore, insulation performance must be improved to reduce the risk of partial discharge. One method to ensure the insulation performance of a transformer is to encapsulate the windings with a plastic mold structure to improve reliability. Mold materials provide higher safety and insulation performance in comparison with conventional transformers, such as oil-filled transformers, due to the use of flame-retardant materials. In addition, the molded transformers are compact and lightweight and, eliminating the requirements of maintenance [5].

However, the molded transformer has a challenge on the cooling performance. In the conventional molded transformer, the windings are enclosed by the plastic mold. Thus, the temperature of the winding rises due to the increased copper loss due to the skin effect and the proximity effect.

This paper proposes providing plastic mold on only in regions with a concentrated electric field around the windings. The experimental results indicate that the temperature rise in the windings is reduced in comparison with the conventional fully molded transformer. Furthermore, the PD test of the transformer demonstrates that the developed transformer possesses sufficient voltage to withstand capability for SST with a 6.6-kV input.

Design of high-frequency transformer for SST

Design of circuit

Fig. 1 illustrates the entire circuit of the assuming SST, featuring the main focus of this paper: a high-frequency transformer. In the paper, ISOP connection with nine cells per phase is assumed for utilization in a 6.6-kV grid. The DC/DC converters in the cell are the current resonant isolated converters. The resonance capacitor is connected in series at the primary side of the transformer. Thus, the current flowing

through the transformer is almost sinusoidal. In this paper, the developed transformer is evaluated with a current resonant DC/DC converter, as shown in Fig. 2.

Electric field distribution

Insulation design in a transformer assuming 6.6-kV input is considered through electric field analysis in FEM. The result of the analysis clarify where insulation materials are required. In this consideration, split structure for the windings is adopted in order to increase the insulation distance. The magnetic core used in the transformer is ferrite. The 16 cores of UU80×150×30N (PC40, TDK) are used from the viewpoint of transformer volume and iron loss.

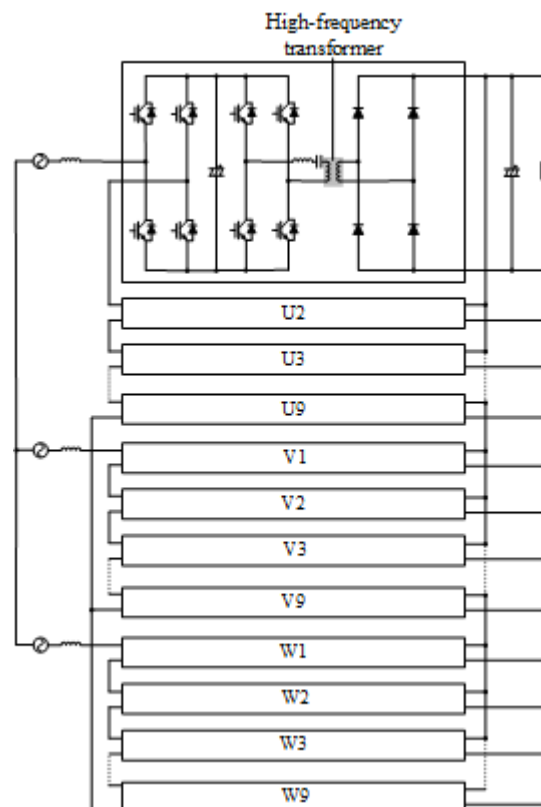


Fig. 1. ISOP connection assuming 6.6 kV system.

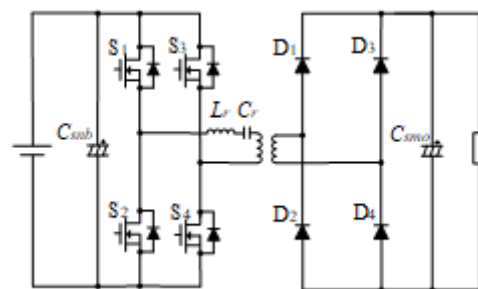


Fig. 2. Current resonant DC/DC converter.

The isolation distance on the high-voltage equipments must be desiend according to the international standard. The requied distance is determined based on a comparable standard for medium-voltage equipment because there are no specific regulations on the isolation distance for high-frequency transformers. The spatial distance is determined based on standard IEC61800-5-1 for adjustable speed electrical power drive systems and IEC60664-1 for insulation coordination for equipment having a rated voltage up to AC 1000 V or DC 1500 V. According to these two standards, an insulation distance of 60.0 mm [6], with a margin of 70.0 mm for this design.

Fig. 3 shows the results of the electric field analysis of the transformer by the finite element analysis (FEM). A peak voltage of 9.33 kV, corresponding to an RMS voltage of 6.6 kV is applied to the primary winding. Fig. 3 (a) shows

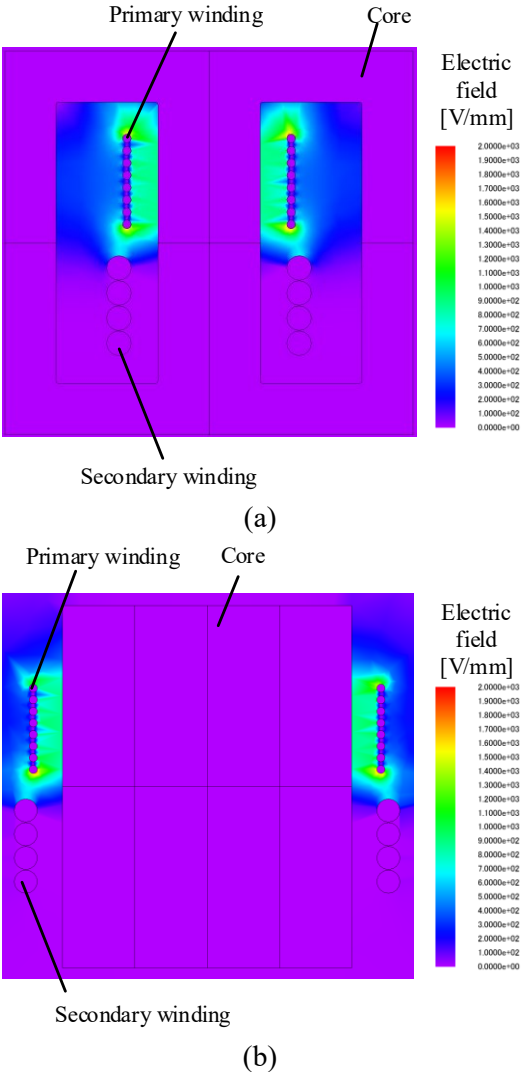


Fig. 3. Electric field distribution in transformer. (a) Front. (b) Side.

the electric field distribution from the front view, while (b) shows it from the side view. The results indicate that electric field concentration occurs between the primary and secondary windings, as well as in the area of electric field concentration between the windings and the core.

Loss Calculation

The iron loss of a transformer can generally be calculated from Steinmetz's equation. Equation (1) is Steinmetz's experimental equation, and the constant is derived from this equation. Here P_i is the iron loss, f is the frequency, B is the magnetic flux density, k , α , and β are Steinmetz coefficients.

$$P_i = kf^\alpha B^\beta \dots\dots\dots (1)$$

The iron loss is calculated by deriving Equation (1) from the core loss waveforms described in the data sheet for PC40. The magnetic flux density B is obtained from equation (2), where N_1 is the number of primary windings, B is magnetic flux flux, V_1 is primary voltage converted to AC, f is frequency, and A_e is the cross-sectional area.

$$B = \frac{V_1}{4fN_1A_e} \dots\dots\dots (2)$$

From equation (2), the magnetic flux density B is 163 mT and the Steinmetz coefficients are $k = 34.24$, $\alpha = 1.22$, $\beta = 1.60$.

In addition, copper loss is calculated by R^2I^2 from the winding resistance of the prototype transformer.

Proposed molded transformer structure

Conventional structure does not allow for forced-air cooling, making the temperature rise of the windings a disadvantage. High-frequency operation raises the temperature because of AC resistance, skin effects, and proximity effects are problems.

In this paper, plastic molding is putting to only the region between the primary and secondary windings, and the area with concentrated electric field region between the windings and the core [7-8]. The bobbin shown in Fig. 5 is designed to implement the proposed structure. The manufacturing process of the bobbin is shown in Fig. 6. The procedure is as follows: (a) Design with 3D CAD (SOLIDWORKS), (b) Generating by 3D printer using heat-resistant ABS material, (c) Inserting urethane material (UF-110-1A, UF-110B mixed) into the cavity of the generated bobbin, and (d) defoaming the mold material under vacuum conditions. The plastic material is

then heated and cured in a thermostatic bath at 85°C or above, which indicates the curing process. The transformer completed through the above process is shown in Fig. 8.

Fig. 8 shows a transformer with a conventional mold structure. The windings are fully enclosed by the plastic mold. Comparative tests will be conducted using this transformer and the transformer of the proposed structure.

Table I shows the parameters of the proposed structure transformer and the conventional structure. The difference in winding resistance

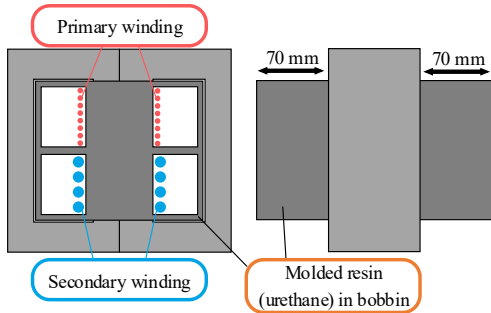


Fig. 5. Proposed transformer's insulation structure.

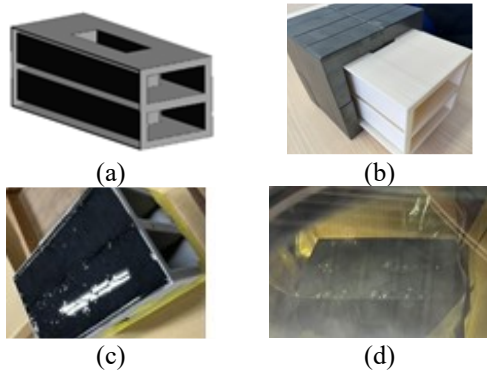


Fig. 6. Creation procedure of bobbin molded transformer. (a) Design in 3D CAD. (b) Printed by 3D printer. (c) Plastic insertion. (d) Vacuum defoaming.

between the conventional and proposed structures is the difference in the type of winding. The conventional structure uses copper plates and the proposed structure uses litz wires.



Fig. 7. The proposed transformer with plastic molding only in the electric field concentration area.



Fig. 8. The conventional transformer with plastic molding over entire winding.

Table I. Transformer parameters.

		Conventional structure	Proposed structure
Primary	Inductance	1.93 mH	1.79 mH
	Winding resistance	160 mΩ	25 mΩ
Secondary	Inductance	484 μH	447 μH
	Winding resistance	40.1 mΩ	7.0 mΩ
Coupling coefficient		0.99	0.95
Winding ratio		8:4	
Power density		12.6 kW/L	

Experimental results

Test results

Table II lists the parameters of the experiment and Fig. 9 shows the prototype of the DC/DC converter. In this paper, the rated power is 37.5 kVA, but this time it is operated at 0.5 p.u. In this test, the design frequency of the transformer is 30 kHz; however, the experiment was conducted at the resonant frequency of 29 kHz. In addition, the current is delayed from the inverter output voltage by approximately 15 deg. to achieve zero-voltage switching.

Fig. 10 shows the operating waveforms of the inverter and transformer. Fig. 10 (a) presents the test results of the conventional structure and (b) shows the test results of the proposed structure. Both waveforms (a) and (b) indicate that the phase of the primary current is delayed in comparison to that of the voltage. These results confirm that zero-voltage switching has been successfully achieved.

Fig. 11 shows the efficiency characteristic of the transformers developed in this study. During

Table II. Circuit parameters.

Parameter		Value
Input voltage	V_{in}	750 V
Output voltage	V_o	375 V
Rated power	S	37.5 kVA
Frequency	f	29 kHz
Resonant inductor	L_r	487 μ H
Resonant capacitor	C_r	56 nF

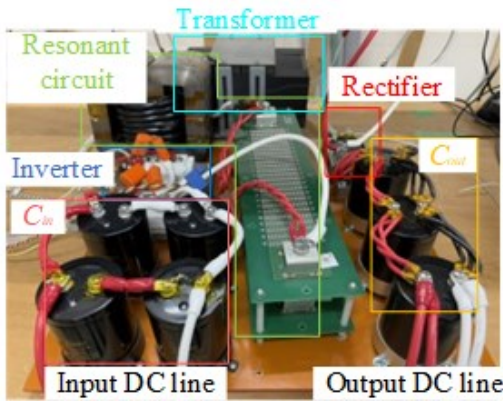


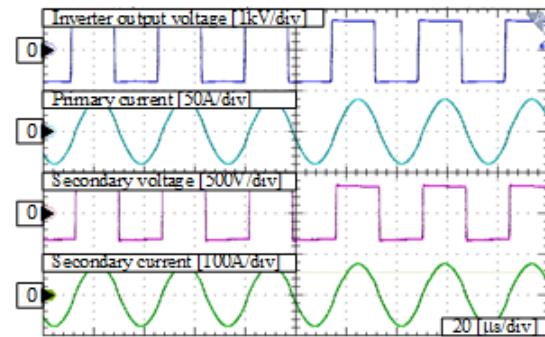
Fig. 9. Test environment of the transformer.

light-load operation, no-load losses dominate, resulting in an efficiency of only about 92%. However, as transmission power increases, the ratio of no-load loss to total loss decreases, and the efficiency near the 0.5 p.u. power reaches up to 99.2% with an output power of 16.5 kW. Note that, the maximum efficiency of the conventional transformer is 98.6% with an output power of 16.8 kW.

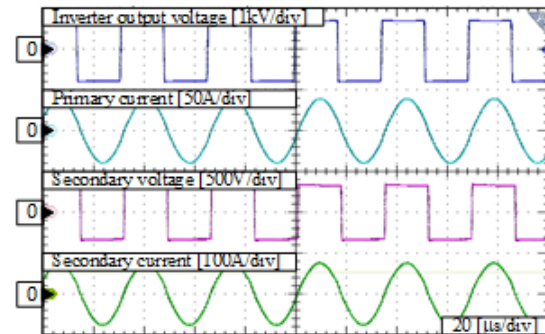
Fig. 12 shows a comparison of the experimental and theoretical losses for the conventional structure. In Fig. 12(b), the measured loss of the proposed structure is 138.5 W, while the theoretical value is 134.6 W, resulting in an error rate of 2.9%. Both results demonstrate that the error rate is below 10%, highlighting the high accuracy of the loss calculation.

Partial discharge test

Fig. 13 shows a circuit diagram of the PD test. The PD measurement setup is shown in Fig. 14. In this test, the discharge threshold is set at 50 pC. The test is then conducted by shorting each winding of the primary and secondary windings. At this time, the insulation performance between



(a)



(b)

Fig. 10. Operating waveforms of the transformer during 0.5 p.u. operation.

(a) Conventional structure.

(b) Proposed structure.

the windings was evaluated at the discharge initiation voltage above the threshold value. The PD tester used in this test is DAC-PD-3 (SOKEN ELECTRIC CO., LTD).

Fig. 15 shows the test results of the PD test, in which Fig. 15 (a) demonstrates the measured result of the proposed mold structure and Fig. 15 (b) demonstrates the measured result of the conventional molded transformer. The results indicate that the proposed structure exhibits a discharge initiation voltage of 7.32 kV, while that of the conventional mold structure reaches up to 9.81 kV. Even though the insulation performance

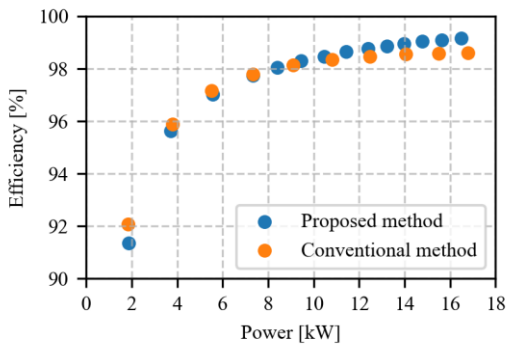
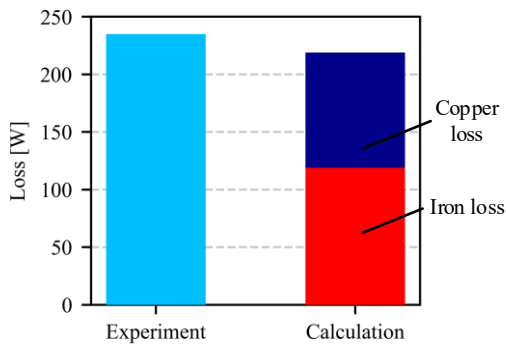
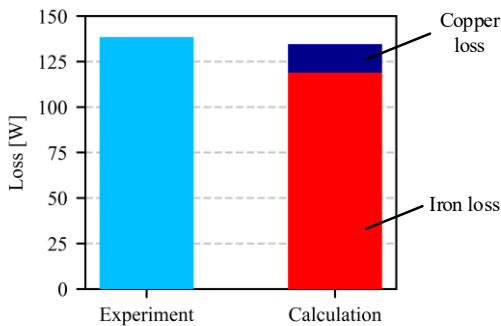


Fig. 11. Efficiency characteristic.



(a)



(b)

Fig. 12. Loss Comparisons.
(a) Conventional molded transformer.
(b) Proposed molded transformer.

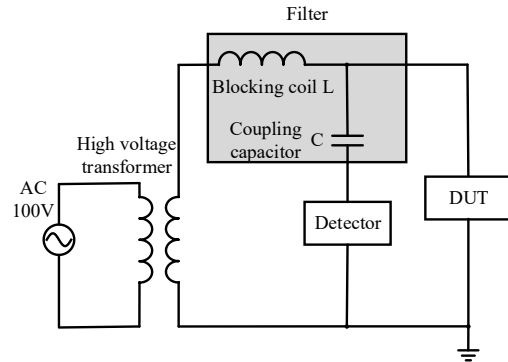


Fig. 13. PD test circuit

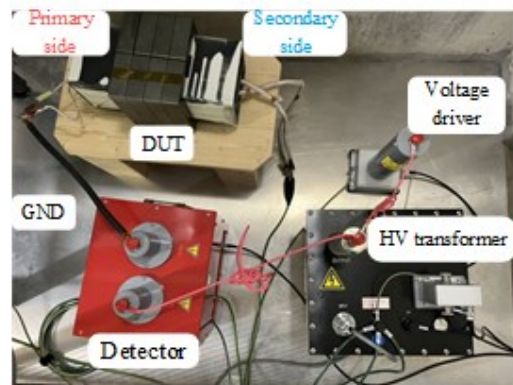
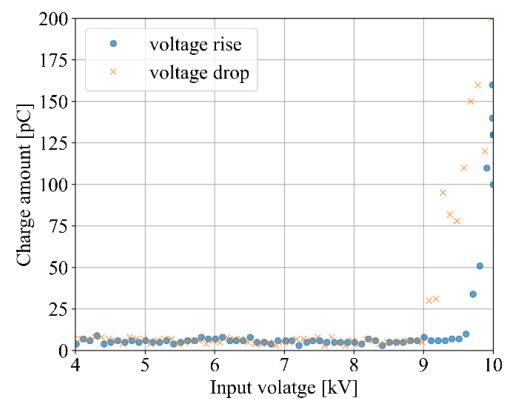
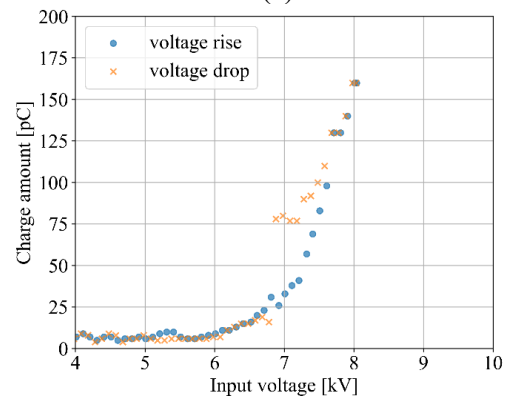


Fig. 14. Test environment for PD test of transformer's prototype.



(a)



(b)

Fig. 15. Test results of partial discharge.
(a) Conventional molded transformer.
(b) Proposed molded transformer.

of the conventional molded transformer is more effective, as the windings are well-insulated by the plastic encasement, the proposed mold structure also achieves excellent insulation performance at 6.6 kV, confirming that it has sufficient insulation performance for the AC grid's specification.

Conclusion

This paper outlines the development of a high-frequency molded transformer for DC/DC converters used in SSTs with an ISOP configuration. The challenge on the conventional high-frequency molded transformers is the increase in the winding temperature caused by higher AC resistance. The mold structure to achieve the forced air-cooling and high-insulation performance is proposed in this paper. The proposed transformer is developed and demonstrated in a DC/DC converter. Based on the test results, it is confirmed that an efficiency of 99.2% can be achieved with a power of 16.5 kW. PD tests are also conducted on the developed transformer, showing that the insulation performance required for a 6.6 kV SST can be achieved. However, the PD test confirmed that the insulation performance is slightly lower than that of the conventional structure.

References

- [1] L. Zheng et al., "Solid-State Transformer and Hybrid Transformer With Integrated Energy Storage in Active Distribution Grids: Technical and Economic Comparison, Dispatch, and Control," in *IEEE Journal of Emerging and Selected Topics in Power Electronics*, vol. 10, no. 4, pp. 3771-3787, Aug. 2022.
- [2] S. A. Saleh et al., "Solid-State Transformers for Distribution Systems—Part II: Deployment Challenges," in *IEEE Transactions on Industry Applications*, vol. 55, no. 6, pp. 5708-5716, Nov.-Dec. 2019.
- [3] G. Ortiz, M. G. Leibl, J. E. Huber and J. W. Kolar, "Design and Experimental Testing of a Resonant DC–DC Converter for Solid-State Transformers," in *IEEE Transactions on Power Electronics*, vol. 32, no. 10, pp. 7534-7542, Oct. 2017.
- [4] E. S. Lee, J. H. Park, M. Y. Kim and J. S. Lee, "High Efficiency Integrated Transformer Design in DAB Converters for Solid-State Transformers," in *IEEE Transactions on Vehicular Technology*, vol. 71, no. 7, pp. 7147-7160, July 2022.
- [5] S. Chen and T. Czaszejko, "Partial discharge test circuit as a spark-gap transmitter," in *IEEE Electrical Insulation Magazine*, vol. 27, no. 3, pp. 36-44, May-June 2011.
- [6] R. Agarwal, H. Li, Z. Guo and P. Cheetham, "The Effects of PWM With High dv/dt on Partial Discharge and Lifetime of Medium-Frequency Transformer for Medium-Voltage (MV) Solid State Transformer Applications," in *IEEE Transactions on Industrial Electronics*, vol. 70, no. 4, pp. 3857-3866, April 2023.
- [7] J. Jiang, W. Chen, Y. Song and Z. Shen, "Active Control Strategy of Partial Discharge for Insulation of High-Power High-Voltage High-Frequency Transformers (H3Ts)," in *IEEE Transactions on Industrial Electronics*, vol. 70, no. 7, pp. 7521-7524, July 2023.
- [8] I. -J. Seo, U. A. Khan, J. -S. Hwang, J. -G. Lee and J. -Y. Koo, "Identification of Insulation Defects Based on Chaotic Analysis of Partial Discharge in HVDC Superconducting Cable," in *IEEE Transactions on Applied Superconductivity*, vol. 25, no. 3, pp. 1-5, June 2015, Art no. 5402005.
- [9] O. Kessler, "The Importance of Partial Discharge Testing: PD Testing Has Proven to Be a Very Reliable Method for Detecting Defects in the Insulation System of Electrical Equipment and for Assessing the Risk of Failure," in *IEEE Power and Energy Magazine*, vol. 18, no. 2, pp. 62-65, March-April 2020.
- [10] L. Niemeyer, "A generalized approach to partial discharge modeling," in *IEEE Transactions on Dielectrics and Electrical Insulation*, vol. 2, no. 4, pp. 510-528, Aug. 1995.
- [11] C. Thirumurugan, G. B. Kumbhar and R. Oruganti, "Effects of impurities on surface discharges at synthetic ester/cellulose board," in *IEEE Transactions on Dielectrics and Electrical Insulation*, vol. 26, no. 1, pp. 64-71, Feb. 2019.
- [12] Z. Guo et al., "A Novel High Insulation 100 kW Medium Frequency Transformer," in *IEEE Transactions on Power Electronics*, vol. 38, no. 1, pp. 112-117, Jan. 2023.
- [13] R. Yonetomi, K. Kusaka, N. Koike and S. Nagai, "Partial Discharge Test of High-frequency Transformers with Plastic Mold for SST," 2024 IEEE 10th International

Power Electronics and Motion Control Conference (IPEMC2024-ECCE Asia), Chengdu, China, 2024, pp. 3007-3012.

- [14] Z. Yi, K. Sun, H. Liu, G. Cao and S. Lu, "Design and Optimization of the Insulation of Medium-Voltage Medium-Frequency Transformers for Solid-State Transformers," in *IEEE Journal of Emerging and Selected Topics in Power Electronics*, vol. 10, no. 4, pp. 3561-3570, Aug. 2022, doi: 10.1109/JESTPE.2021.3094674.
- [15] Z. Guo et al., "A Novel High Insulation 100 kW Medium Frequency Transformer," in *IEEE Transactions on Power Electronics*, vol. 38, no. 1, pp. 112-117, Jan.